Available online at www.sciencedirect.com
ScienceDirect
Trans. Nonferrous Met. Soc. China 19(2009) 681−685
Transactions of Nonferrous Metals Society of China
www.tnmsc.cn

Partial phase relationships of Mg-Zn-Ce system at 350 ℃

HUANG Ming-li(黄明丽)[1,2], LI Hong-xiao(李洪晓)[1], DING Hua(丁 桦)[1],
REN Yu-ping(任玉平)[1], QIN Gao-wu(秦高梧)[1], HAO Shi-ming(郝士明)[1]

1. Key Laboratory for Anisotropy and Texture of Materials (Ministry of Education), School of Materials and Metallurgy, Northeastern University, Shenyang 110004, China;
2. Department of Materials Science and Engineering, Northeastern University (Qinhuangdao), Qinhuangdao 110004, China

Received 23 September 2008; accepted 9 January 2009

Abstract: The alloys were prepared in Mg-rich corner of Mg-Zn-Ce system. Partial phase equilibrium relationships of these alloys at 350 ℃ were identified by using scanning electron microscopy(SEM), electron probe microanalysis(EPMA), X-ray diffraction(XRD) analysis and selected area electron diffraction(SAED) pattern analysis of transmission electron microscopy(TEM). Partial isothermal section of Mg-Zn-Ce system in Mg-rich corner was identified. The results show that there is one ternary compound (*T*-phase) in Mg-Zn-Ce system. The *T*-phase is a linear ternary compound in which the content of Ce is about 7.7% (molar fraction); while the content of Zn is changed from 19.3% to 43.6% (molar fraction). The crystal structure of *T*-phase is C-centered orthorhombic. In addition, one two-phase region of Mg+*T*-phase and one three-phase region of Mg+*T*-phase+MgZn(Ce) exist in the Mg-rich corner of Mg-Zn-Ce system at 350 ℃.

Key words: Mg-Zn-Ce system; phase equilibrium; two-phase region; three-phase region; *T*-phase

1 Introduction

Magnesium alloys are one kind of the lightest structural metal materials, and its application potential in automobile industry, aviation industry and electron industry is focused[1−3]. But compared with steel and aluminum alloy, the application process of magnesium alloys is limited because of the poor plastic property at room temperature and the poor creep resistant property at an elevated temperature. So, the development of magnesium alloys with high mechanical properties, especially at elevated temperature is crucial for application[4−6]. The addition of rare earth element can not only refine the crystal grain, but also improve the creep resistance at elevated temperature, because of the formation of high melting-point compounds[7−8]. For Mg-Zn-RE system, it is the same reason[9−12].

Phase diagram is the basis of alloy design. Up to now, the binary systems of Ce-Mg, Mg-Zn and Ce-Zn are perfect[13], but the information of the Mg-Zn-Ce ternary system is limited. There are only two longitudinal sections now, and some information about the compound is not clear[14−15]. So, it is important to perfect the phase information of the Mg-Zn-Ce system. Therefore, the phase relationships of the Mg-Zn-Ce system in Mg-rich corner at 350 ℃ were studied in this work.

2 Experimental

The Mg-Zn-Ce alloys with nominal composition shown in Table 1 were prepared by repeated melting. The purity of Mg and the purity of Zn were 99.99%, and the purity of Ce was about 99.8%. Each sample ingot was about 30 g. The pure metals of each group were mixed together, and then put into the carbon crucible in a vacuum induction furnace under Ar atmosphere, followed by furnace cooling. Then the samples were wrapped with tantalum foils respectively and sealed in a quartz tube under the vacuum of 10^{-3} Pa and annealed at 350 ℃ for 1 440 h, followed by water cooling. Phase identification and lattice parameter determination were made by X-ray diffractometry(XRD) using Siemens D5000 diffractometer with Cu K_α radiation, a voltage of 40 kV and a current of 40 mA. Microstructures of samples were studied by scanning electron microscopy

Foundation item: Project(50471025) supported by the National Natural Science Foundation of China; Project(20052028) supported by the Natural Science Foundation of Liaoning Province, China; Project(2006BAE04B09-7) supported by the National Key Technology R&D Program during the 11th Five-Year Plan Period
Corresponding author: HUANG Ming-li; Tel: +86-24-83672241; E-mail: mingli_huang@126.com
DOI: 10.1016/S1003-6326(08)60333-7

Table 1 EPMA data of equilibrium phases in alloys (molar fraction, %)

Nominal composition of alloys	Mg solid solution			*T*-phase			MgZn phase		
	Mg	Zn	Ce	Mg	Zn	Ce	Mg	Zn	Ce
$Mg_{80}Zn_{15}Ce_5$	99.3	0.7	0	73.0	19.3	7.7		−	
$Mg_{86}Zn_{10.5}Ce_{3.5}$	99.3	0.7	0	73.0	19.4	7.6		−	
$Mg_{75}Zn_{20}Ce_5$	98.3	1.7	0	61.6	30.5	7.9		−	
$Mg_{70}Zn_{25}Ce_5$	98.1	1.9	0	57.7	34.5	7.8		−	
$Mg_{58}Zn_{37}Ce_5$	96.9	3.1	0	49.2	43.0	7.8	55.3	43.3	1.4
$Mg_{81}Zn_{17.5}Ce_{1.5}$	97.0	3.0	0	48.8	43.6	7.6	56.0	42.5	1.5

(SEM) using SSX-550 microscope. The compositions of equilibrium phases in alloys were analyzed on electron probe microanalyzer(EPMA) with a beam size of 1 μm and a voltage of 15 kV. The highly pure Mg, Zn and Ce were served as standards to revise the characteristic radiations, and the purities of them were 99.99%, 99.99% and 99.8%, respectively. The selected area electron diffraction(SAED) of the intermetallic phases was carried out on TECNAI $G^2$20 transmission electron microscope(TEM) operated at 200 kV.

3 Results and discussion

3.1 Equilibrium of *T*-phase+*α*(Mg)

The microstructures of the alloys of $Mg_{80}Zn_{15}Ce_5$, $Mg_{86}Zn_{10.5}Ce_{3.5}$ and $Mg_{70}Zn_{25}Ce_5$ are shown in Fig.1. All alloys consist of two phases with similar microstructures. The black is Mg matrix which contains a little Zn as shown in Table 1. The bright phase in each alloy is a ternary compound. Table 1 shows that the contents of Zn of the ternary compounds in different alloys are from 19.3% to 43.6%, but the content of Ce is about 7.7%, which has no change, showing the ternary compounds have linear characterization in their compositions. The results suggest that the increasing of Zn in the ternary compounds should be based on the substitution of Mg by it.

Fig.2(a) shows the XRD patterns of the three alloys of $Mg_{80}Zn_{15}Ce_5$, $Mg_{86}Zn_{10.5}Ce_{3.5}$ and $Mg_{70}Zn_{25}Ce_5$. According to the results of Table 1 and Fig.1, the diffraction peaks of each diffraction pattern in Fig.2(a) must consist of the peaks of ternary compound and Mg. It is well known that the structure and diffraction peaks of Mg have been clear now, and the peaks of Mg can be indexed easily by the standard of PDF card. Therefore, except the diffraction peaks of Mg, the rest should be assigned to the ternary compound for each XRD diffraction pattern. Fig.2(a) also shows that the XRD diffraction patterns have the nearly one-to-one correspondence diffraction peaks to each other, that is to say, the diffraction peaks of the ternary compound in each alloy diffraction pattern are one-to-one correspondence. This suggests that the ternary compounds in the three alloys have the same crystal structure. The characterizations of composition and the crystal structure of the ternary compounds support them

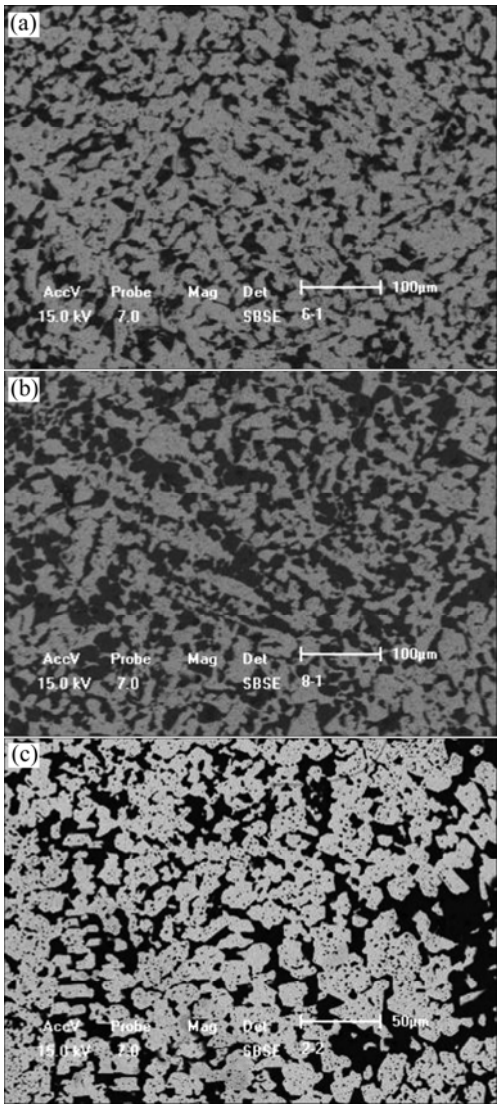

Fig.1 Microstructures of two-phase equilibrium alloys: (a) $Mg_{80}Zn_{15}Ce_5$; (b) $Mg_{86}Zn_{10.5}Ce_{3.5}$; (c) $Mg_{70}Zn_{25}Ce_5$ (Bright is *T*-phase, black is Mg matrix)

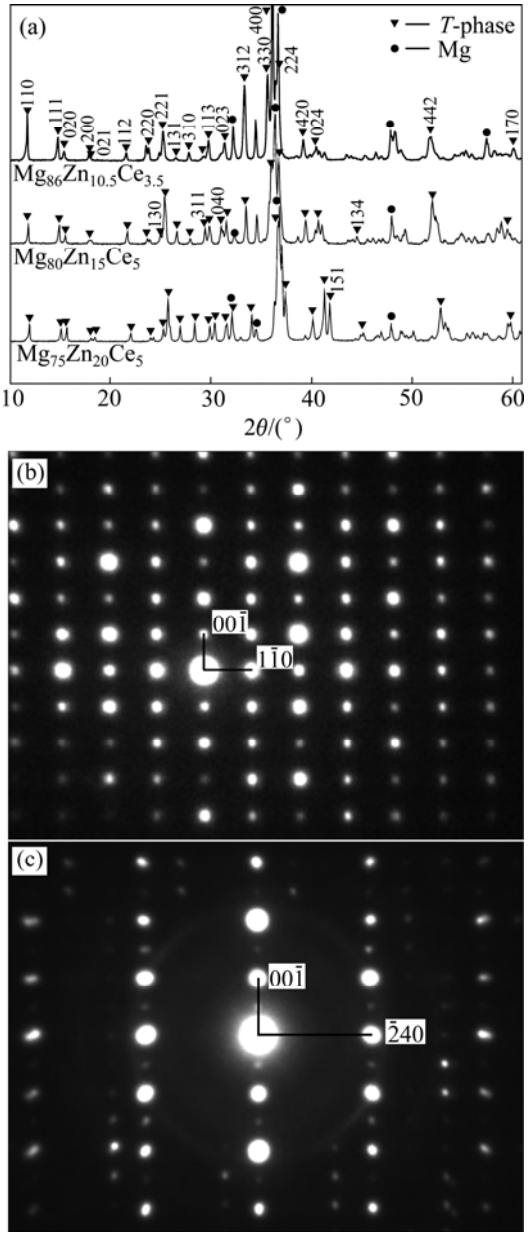

Fig.2 XRD patterns of two-phase equilibrium alloys (a), SAED patterns of *T*-phase taken from [110] zone axis (b) and [210] zone axis (c)

to be looked as one linear ternary compound, which is one linear ternary compound here called as *T*-phase.

By calculating and simulating the data of the diffraction peaks, the C-centered crystal structure of *T*-phase is identified. According to the Brgg formula: $2d\sin\theta=\lambda$, the formula of the interplanar crystal spacing for the orthorhombic system: $d=1/\sqrt{\frac{h^2}{a^2}+\frac{k^2}{b^2}+\frac{l^2}{c^2}}$ and the condition for extinction of C-centered crystal lattice: $h+k=2n+1$ (n is integer), the Miller indices of each diffraction peak of *T*-phase can be determined. Fig.2(b) shows the SAED pattern of *T*-phase taken from [110] zone axis and Fig.2(c) shows the SAED pattern taken from [210] zone axis. Figs.2(b) and (c) suggest furthermore that the crystal lattice of *T*-phase is C-centered orthorhombic.

3.2 Three-phase equilibrium of *α*(Mg)+MgZn(Ce)+*T*-phase at 350 ℃

Fig.3 shows the typical microstructures of three-phase equilibrium alloys. The black is Mg matrix, in which solubility of Zn is about 3.0% at 350 ℃. The grey is similar to MgZn phase, but there contains 1.5% Ce in it. According to Mg-Zn binary diagram, the melting point of MgZn is 347 ℃ and solidification of MgZn phase should disappear at 350 ℃ theoretically[13]. Therefore, the existence of MgZn at the solid state of 350 ℃ is owing to its solubility of 1.5% Ce, which is a high melting temperature element, and the grey phase is called as MgZn(Ce) here. The bright is *T*-phase, which contains about 44%Zn, about 8%Ce and balanced Mg.

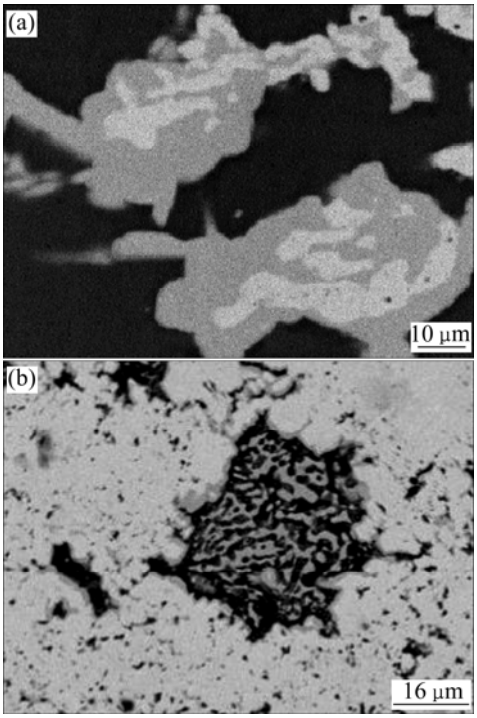

Fig.3 Microstructures of three-phase equilibrium alloys: (a) $Mg_{81}Zn_{17.5}Ce_{1.5}$, (b) $Mg_{58}Zn_{37}Ce_5$ (Bright is *T*-phase, grey is MgZnCe and black is Mg matrix)

Fig.4(a) shows the XRD patterns of $Mg_{81}Zn_{17.5}Ce_{1.5}$ alloy and $Mg_{80}Zn_{15}Ce_5$ alloy, and Fig.4(b) shows the SAED pattern of *T*-phase in $Mg_{81}Zn_{17.5}Ce_{1.5}$ alloy taken from [012] zone axis. The results of Fig.4 show that the *T*-phase in $Mg_{81}Zn_{17.5}Ce_{1.5}$ alloy also has a C-centered crystal structure. In Fig.2, the XRD pattern of $Mg_{80}Zn_{15}Ce_5$ alloy has been discussed and it is

introduced in Fig.4(a) to show the characterization of the peaks of *T*-phase in two-phase equilibrium and three-phase equilibrium. For the XRD pattern of $Mg_{81}Zn_{17.5}Ce_{1.5}$ alloy, except the peaks of Mg matrix and MgZn(Ce), the rest peaks are the diffraction peaks of *T*-phase. Fig.4(a) shows that the peaks of *T*-phase in $Mg_{81}Zn_{17.5}Ce_{1.5}$ alloy also correspond to those in $Mg_{80}Zn_{15}Ce_5$ alloy. But if comparing the peak data in Fig.2(a) with Fig.4(a) of *T*-phase carefully, it is shown that for each group corresponding peaks, the values of 2θ shift to higher with the increasing of Zn content in the *T*-phase regularly. This suggests that with the increase of Zn content, the crystal structure of *T*-phase has no change.

The reason that the values of 2θ change with the increase of Zn content in the *T*-phase is known as that the radius of Zn is 0.153 nm, which is 0.019 nm shorter than that of Mg. When the content of Ce is not changed, the lattice parameters of *T*-phase should be decreased with Mg content being substituted by Zn content successively. According to the formula of Brgg and the formula of interplanar of the orthorhombic system, the formula, $2\theta=2\arcsin\frac{\lambda}{2}\sqrt{\frac{h^2}{a^2}+\frac{k^2}{b^2}+\frac{l^2}{c^2}}$ can be obtained. This equation shows that, for each (h k l) triplet, the values of 2θ shift to higher with the decreasing of parameters. That is to say, with the increasing of Zn content, the 2θ values shift to higher. So, the theoretic analysis is consistent with the result of Fig.4(a) and Fig.2.

According to the analysis above, the *T*-phase is a linear compound. And the crystal lattice is C-centered orthorhombic. With Mg content being substituted by Zn content, the lattice parameters should decrease a little regularly.

3.3 Partial isothermal section of Mg-Zn-Ce system

According to the results above, the partial isothermal section of Mg-Zn-Ce system in Mg-rich corner at 350 ℃ is determined, as shown in Fig.5. *T*-phase is a stable solid phase at 350 ℃, and has two-phase equilibrium with Mg solid solution in the wide composition range and the linear characterization of

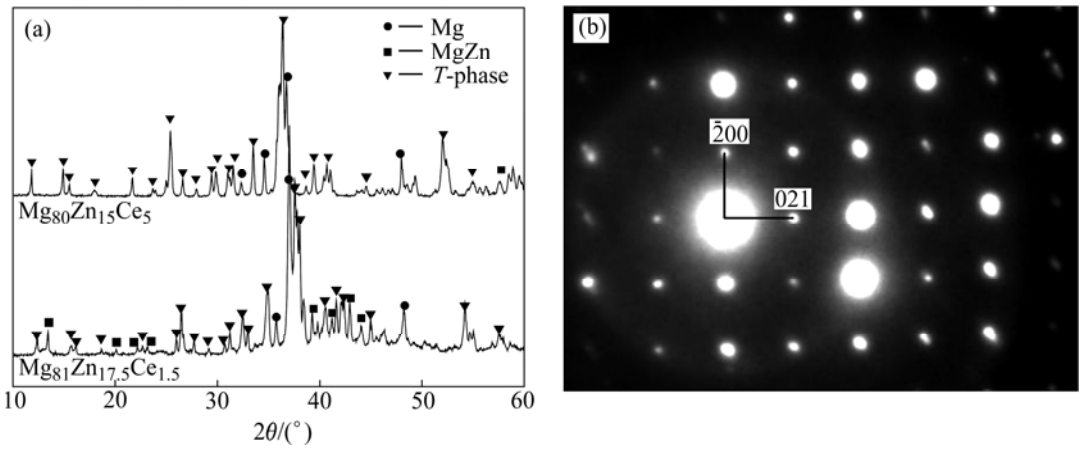

Fig.4 Comparison of XRD patterns of $Mg_{81}Zn_{17.5}Ce_{1.5}$ alloy and $Mg_{80}Zn_{15}Ce_5$ alloy (a), and SAED pattern of *T*-phase in $Mg_{81}Zn_{17.5}Ce_{1.5}$ alloy taken from [012] zone axis (b)

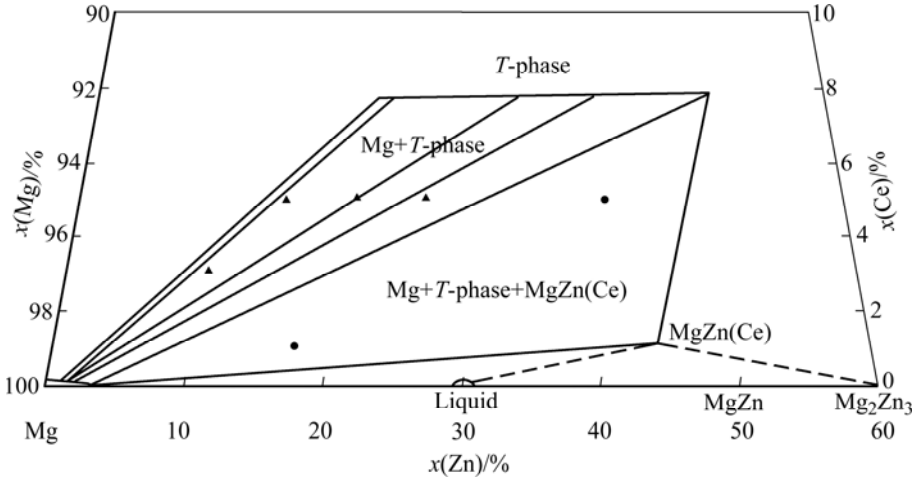

Fig.5 Partial isothermal section of Mg-Zn-Ce system at 350 ℃

it can be seen clearly in Fig.5. The three-phase region of Mg+*T*-phase+MgZn(Ce) also exists near the wide two-phase region. According to the knowledge of Mg-Zn binary system, the three-phase region of *L*+MgZn(Ce)+Mg_2Zn_3 can be deduced.

4 Conclusions

1) There exists a linear ternary *T*-phase in Mg-rich corner of Mg-Zn-Ce system with the compositions of 7.7% Ce, 19.3%−43.6% Zn and balanced Mg at 350 ℃.

2) The diffraction pattern of *T*-phase is determined and its crystal lattice type is C-centered orthorhombic. With the increasing of Zn, the lattice parameters of *T*-phase decrease.

3) There exist a two-phase equilibrium of *T*-phase+*α*(Mg) and a three-phase equilibrium of *α*(Mg)+MgZn(Ce)+*T*-phase in the Mg-rich corner of Mg-Zn-Ce system at 350 ℃.

References

[1] BONDAREV B I, BESSONOV A M. Metallurgical achievements in the field of production and application of magnesium alloys [J]. Tsvetnye Metally, 2005(5/6): 131−134 .

[2] SCHUMANN S, FRIEDRICH H. Current and future use of magnesium in the automobile industry [J]. Materials Science Forum, 2003, 419/422: 51−56.

[3] FANG Can-feng, ZHANG Xing-guo, YU Yan-hao, JIN Jun-ze. Properties and forming technology of magnesium alloys and its application [J]. Heat Treatment of Metals, 2006, 31(3): 12−16.

[4] BRONFIN B, KATSIR M, YOSEF O B, MOLL F, SCHUMANN S. Metallurgical background to the development of creep resistant gravity casting magnesium alloys [C]// Magnesium Technology 2005, Proceedings of the Symposium Sponsored by the Magnesium Committee of the Light Metals Division (LMD) of TMS with the International Magnesium Association. Warrendale: Minerals, Metals & Materials Society, 2005: 395−401.

[5] AGHION E, BRONFIN B, von BUCH F, SCHUMANN S, FRIEDRICH H. Dead sea magnesium alloys newly developed for high temperature applications [C]// Magnesium Technology 2003 Symposium. Warrendale: TMS, 2003: 177−82.

[6] AGHION E, BRONFIN B, ELIEZER D, von BUCH F, SCHUMANN S, FRIEDRICH H. The art of developing new magnesium alloys for high temperature applications [J]. Materials Science Forum, 2003, 419/422: 407−418.

[7] BAKKE P, WESTENGEN H. The role of rare earth elements in structure and property control of magnesium die casting alloys [C]// Magnesium Technology 2005, Proceedings of the Symposium Sponsored by the Magnesium Committee of the Light Metals Division (LMD) of TMS with the International Magnesium Association. Warrendale: Minerals, Metals & Materials Society, 2005: 291−296.

[8] OMORI G, MATSUO S, ASADA H. Precipitation process in a Mg-Ce alloy [J]. Transactions of the Japan Institute of Metals, 1975, 16(5): 247−255.

[9] YU Kun, LI Wen-xian, WANG Ri-chu. Mechanical properties and microstructure of as-cast and extruded Mg-(Ce,Nd)-Zn-Zr alloys [J]. Journal of Central South University of Technology: English Edition, 2005, 12(5): 499−502.

[10] WEI L Y, DUNLOP G L, WESTENGEN H. Precipitation hardening of Mg-Zn and Mg-Zn-RE alloys [J]. Metallurgical and Materials Transactions, 1995, 26A(7): 1705−1716.

[11] LI Qiang, WANG Qu-dong, WANG Ying-xin, ZENG Xiao-qin, DING Wen-jiang. Effect of Nd and Y addition on microstructure and mechanical properties of as-cast Mg-Zn-Zr alloy [J]. Alloys and Compounds, 2007, 427: 115−123.

[12] JUN J H, PARK B K, KIM J M, KIM K, UNG W J. Microstructures and mechanical properties of Mg-Zn-RE-Ca casting alloys [J]. Materials Science Forum, 2006, 510/511: 214−217.

[13] MASSALSKI T B, OKAMOTO H, SUBRAMANIAN P R, KACPRZAK L. Binary alloy phase diagrams [M]. 2nd ed. Orlando: ASM International, 1996.

[14] DRITS M E, DROZDOVA E I, KOROL'KOVA I G, KINZHIBALO V V, TYVANCHUK A T. Investigation of polythermal sections of the Mg-Zn-Ce system in the Mg-rich region [J]. Russian Metallurgy: Engl Trans, 1989, 2: 195−197.

[15] VILLARS P, PRINCE A, OKAMOTO H. Handbook of ternary alloy phase diagrams [M]. Orlando: CD-ROM, ASM International, 1997.

(Edited by YANG Hua)